

Supporting Information

Comparing direct pyrolysis and post-impregnation in the synthesis of atomic Fe active sites for solvent-free aerobic coupling of benzylamine

Guilong Lu ¹, Zewen Shen ², Philipp Schwiderowski ¹, Jannik Böttger ¹, Tim Herrendorf ³, Wolfgang Kleist ³, Xiaoyu Li ¹, Guixia Zhao ², Baoxiang Peng ¹, Xiubing Huang ^{4*}, Martin Muhler ^{1*}

¹ Laboratory of Industrial Chemistry, Ruhr University Bochum, 44780 Bochum, Germany

² North China Electric Power University, 102206 Beijing, PR China

³ Fachbereich Chemie, RPTU Kaiserslautern-Landau, 67663 Kaiserslautern, Germany

⁴ Beijing Key Laboratory of Function Materials for Molecule & Structure Construction, University of Science and Technology Beijing, 100083 Beijing, PR China

1. Material Preparation

1.1. Materials

Unless otherwise noted, all reagents were obtained from Sigma-Aldrich or Alfa Aesar and used as received without further purification.

1.2. Synthesis of the mesoporous silica template

The SiO₂ nanosphere was prepared according to a previously reported method based on the Stöber method. Typically, 10 mL of tetraethyl orthosilicate (TEOS) was added to 50 mL of ethanol with vigorous stirring to form solution A, meanwhile, 10 mL of aqueous ammonia and 20 mL of deionized water were added to 50 mL of ethanol with vigorous stirring to form solution B. After solution A was heated to 40 °C, solution B was added to solution A dropwise. The mixture was kept stirring at 40 °C for 2.5 h to obtain the uniform SiO₂ nanospheres (SiO₂ core). Then, a mixture solution of 10 mL TEOS, 5g polyvinylpyrrolidone (PVP) K30 (M_w ~ 40000), and 10 mL ethanol was added dropwise to the above silica sol with vigorous stirring at 40 °C for 2 h to form the mesoporous SiO₂ shell. After cooling to room temperature, the mixed solution was centrifuged to construct the ordered structure and then dried at 80 °C overnight. The dried ordered SiO₂ template was calcinated at 700 °C for 6 h in the air to remove PVP and obtain the mesoporous shell (SiO₂ template yield: ~ 11 g).

2. Characterization results

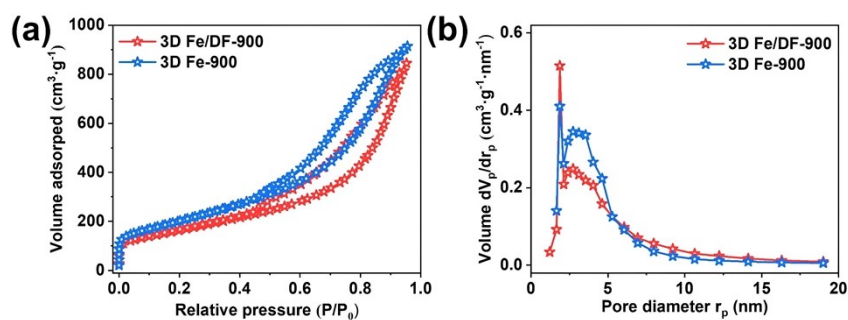


Fig. S1 (a) N_2 sorption isotherms and (b) pore size distributions of 3D Fe/DF-900 and 3D Fe-900.

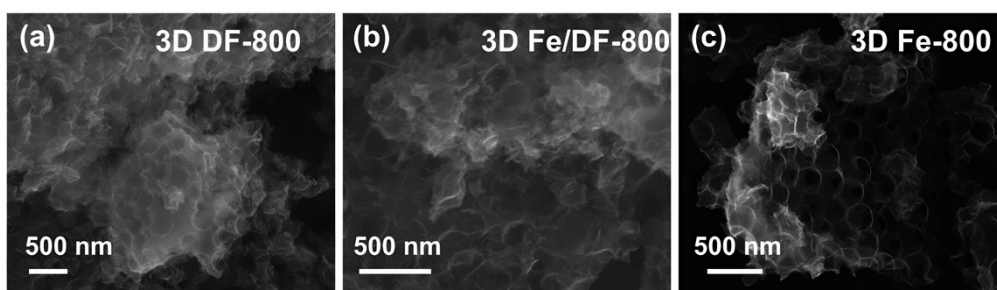


Fig. S2 SEM images of (a) 3D DF-800, (b) 3D Fe/DF-800, and (c) 3D Fe-800.

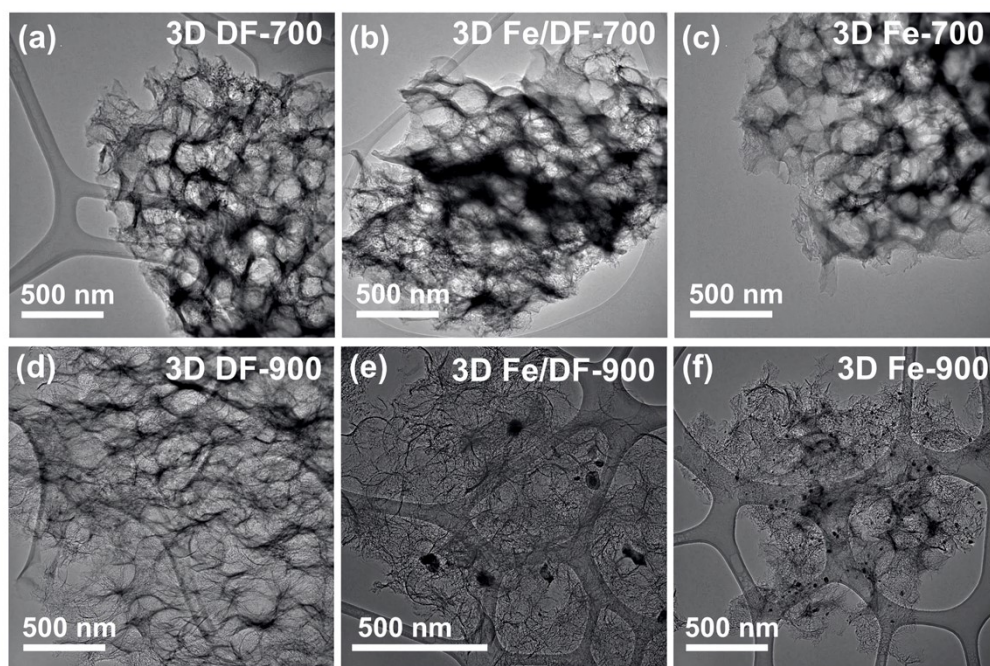


Fig. S3 TEM images of the (a) 3D DF-700, (b) 3D Fe/DF-700, (c) 3D Fe-700, (d) 3D DF-900, (e) 3D Fe/DF-900, and (f) 3D Fe-900.

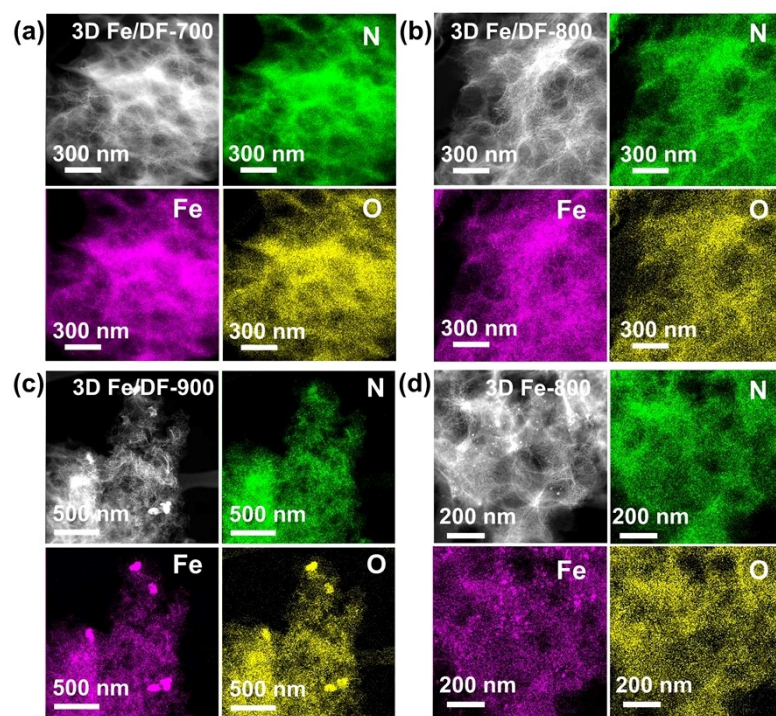


Fig. S4 EDS elemental mapping of N, Fe and O atoms for (a) 3D Fe/DF-700, (b) 3D Fe/DF-800, (c) 3D Fe/DF-900 and (d) 3D Fe-800.

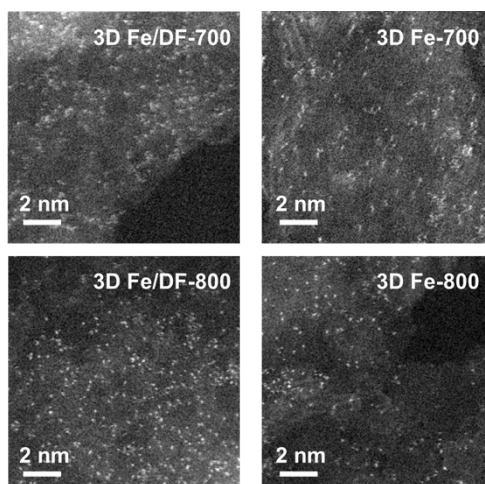


Fig. S5 AC-HAADF-STEM images of the (a) 3D Fe/DF-700, (b) 3D Fe-700, (c) 3D Fe/DF-800, and (d) 3D Fe-800.

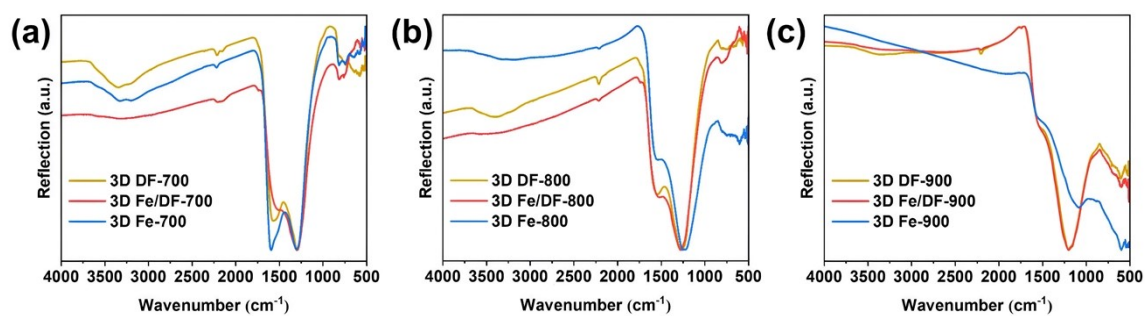


Fig. S6 IR spectra of the 3D DF-X supports, 3D Fe/DF-X, and 3D Fe-X catalysts.

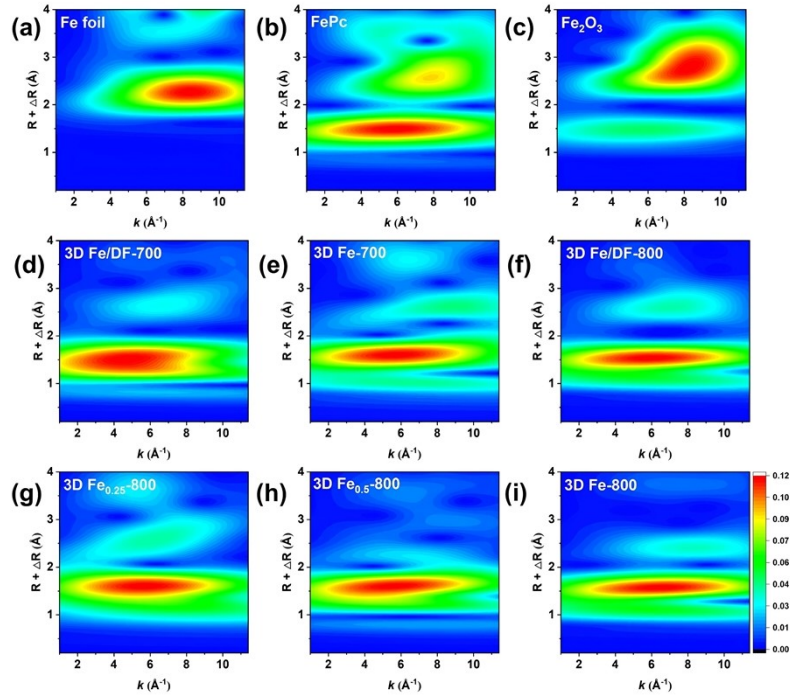


Fig. S7 The wavelet transform contour plots of the k^3 -weighted EXAFS data of (a-c) the reference samples, (d) 3D Fe/DF-700, (e) 3D Fe-700, (f) 3D Fe/DF-800, (g) 3D Fe_{0.25}-800, (h) 3D Fe_{0.5}-800, and (i) 3D Fe-800.

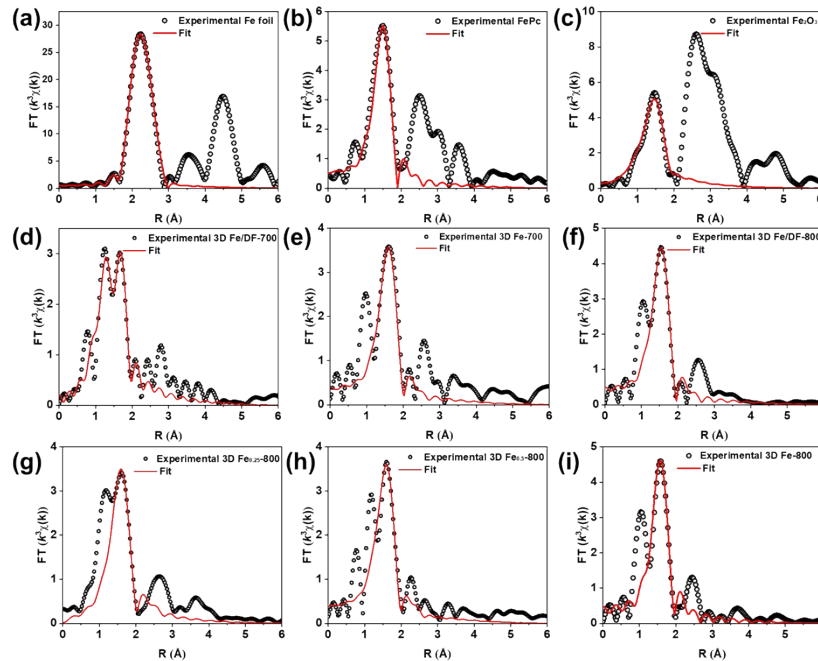


Fig. S8 Fourier transforms of Fe K-edge EXAFS and corresponding fitting curves of (a-c) the reference samples, (d) 3D Fe/DF-700, (e) 3D Fe-700, (f) 3D Fe/DF-800, (g) 3D Fe_{0.25}-800, (h) 3D Fe_{0.5}-800, and (i) 3D Fe-800 in R space.

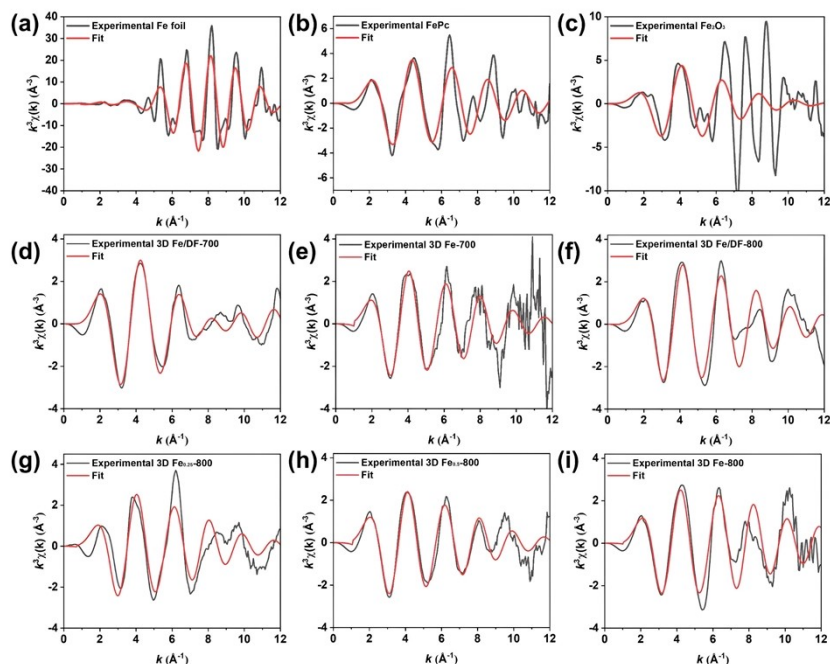


Fig. S9 Fourier transforms of Fe K-edge EXAFS and corresponding fitting curves of (a-c) the reference samples, (d) 3D Fe/DF-700, (e) 3D Fe-700, (f) 3D Fe/DF-800, (g) 3D Fe_{0.25}-800, (h) 3D Fe_{0.5}-800, and (i) 3D Fe-800 in K space.

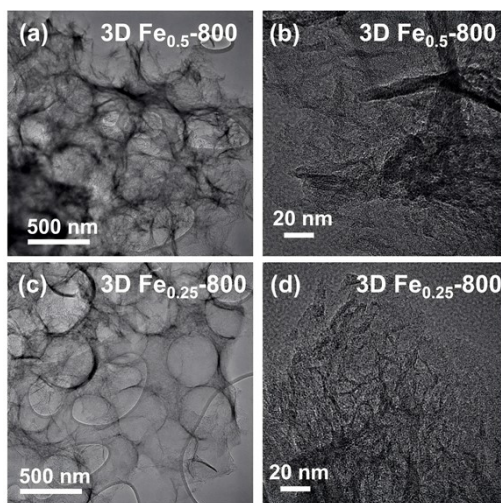


Fig. S10 TEM images and HR-TEM images of (a-b) 3D Fe_{0.5}-800 and (c-d) 3D Fe_{0.25}-800.

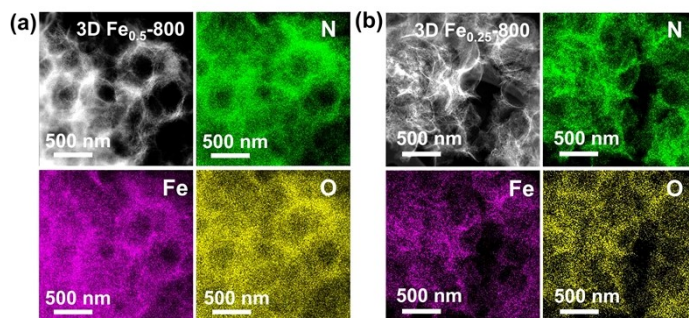


Fig. S11 EDS elemental mapping of N, Fe, and O atoms for (a) 3D Fe_{0.5}-800 and (b) 3D Fe_{0.25}-800.

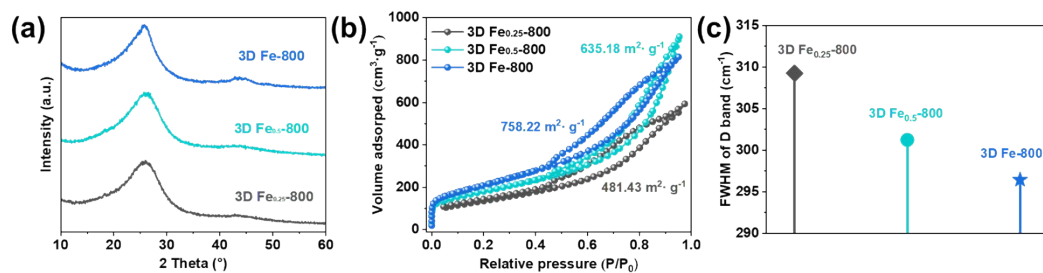


Fig. S12 (a) XRD patterns, (b) N₂ sorption isotherms and (c) the full width at half maximum of the carbon D band of 3D Fe_{0.25}-800, 3D Fe_{0.5}-800, and 3D Fe-800.

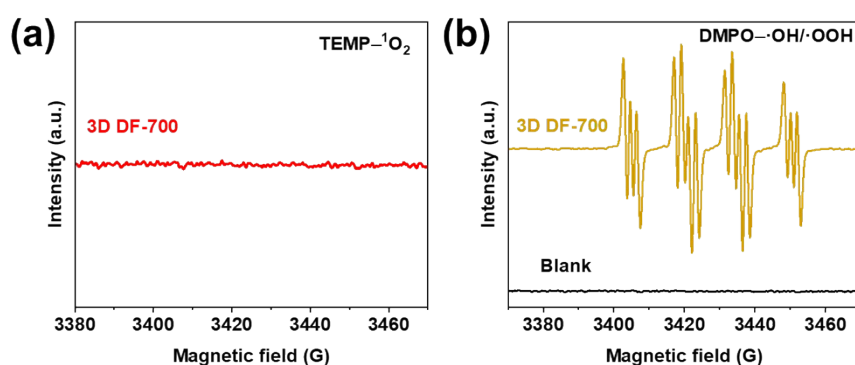


Fig. S13 EPR signals of (a) TEMP-¹O₂ adduct, and (b) DMPO-[•]OH/[•]OOH adducts in the presence of 3D DF-700 at 110 °C.

Table S1 Specific surface areas and pore volumes of 3D Fe/DF-X series catalysts, 3D Fe-X series catalysts, and 3D DF-800 carbon support.

Sample	BET Surface area (m ² /g)	BJH Pore volume (cm ³ /g)
3D Fe/DF-700	169	0.324
3D Fe-700	308	0.376
3D Fe/DF-800	448	0.919
3D Fe-800	758	1.258
3D Fe/DF-900	590	1.312
3D Fe-900	731	1.373
3D DF-800	501	1.049

Table S2 Fe loadings determined by ICP-OES and EDS.

Entry	Sample	Fe Content ^{a)} (wt.%)	Fe Content ^{b)} (wt.%)
1	3D Fe/DF-700	7.09	4.92
2	3D Fe-700	1.48	0.91
3	3D Fe/DF-800	6.70	3.58
4	3D Fe-800	3.97	1.48
5	3D Fe/DF-900	6.20	2.55
6	3D Fe-900	3.31	1.01
7	3D Fe _{0.5} -600-800	3.51	1.68
8	3D Fe _{0.25} -600-800	3.28	1.35

^{a)} Measured by ICP-OES; ^{b)} Measured by EDS.

Table S3 Chemical compositions derived from XPS results.

Entry	Sample	C (% on surface)	N (% on surface)	Fe (% on surface)	O (% on surface)
1	3D DF-700	39.9	37.0	-----	23.1
2	3D Fe/DF-700	32.1	26.7	28.2	13.00
3	3D Fe-700	62.6	34.0	0.6	2.8
4	3D DF-800	49.9	30.6	-----	19.5
5	3D Fe/DF-800	38.4	21.1	25.4	15.0
6	3D Fe-800	75.4	18.1	1.2	5.3
7	3D DF-900	60.5	22.5	-----	17.0
8	3D Fe/DF-900	51.6	16.4	16.3	15.8
9	3D Fe-900	85.7	6.9	0.7	6.7
10	3D Fe _{0.5} -800	66.5	27.2	1.0	5.4
11	3D Fe _{0.25} -800	67.0	26.5	1.1	5.5

Table S4 EXAFS fitting parameters at the Fe K-edge.

Sample	First shell	N ^{a)}	R (Å) ^{b)}	σ^2 (Å ² ·10 ⁻³) ^{c)}	ΔE (eV) ^{d)}	R factor (%)
Fe foil	Fe-Fe	8.0	2.48	4.95	3.3	0.2
Fe ₂ O ₃	Fe-O	3.0	1.96	7.25	3.5	0.3
FePc	Fe-N	4.0	1.92	8.01	1.9	0.2
3D Fe/DF-700	Fe-N	1.0	1.93	5.23	1.5	0.3
	Fe-O	3.1	1.97	3.09	5.2	
3D Fe-700	Fe-N	4.0	1.94	10.0	3.9	0.2
3D Fe/DF-800	Fe-N	3.2	1.93	3.31	1.2	0.3
	Fe-O	1.0	1.97	6.83	4.6	
3D Fe-800	Fe-N	3.1	1.93	5.8	4.0	0.2
3D Fe _{0.5} -600-800	Fe-N	3.8	1.94	10.0	4.5	0.2
3D Fe _{0.25} -600-800	Fe-N	3.0	1.93	3.52	4.2	0.1
	Fe-O	1.0	1.97	5.89	5.9	

^{a)} N: coordination numbers (CN); ^{b)} R: bond distance; ^{c)} σ^2 : Debye-Waller factors; ^{d)} ΔE_0 : the inner potential correction; R factor: goodness of fit; S_0^2 was set as 0.95 for all prepared catalysts, which was obtained from the experimental EXAFS fit of the reference FePc by fixing CN as the known crystallographic value and was fixed to all the samples; Note: the error range of N and σ^2 is within 20%, and the accuracy range for R is within ± 0.04 Å.

Table S5 Catalytic performances of different catalysts in the oxidative coupling of benzylamine.^a

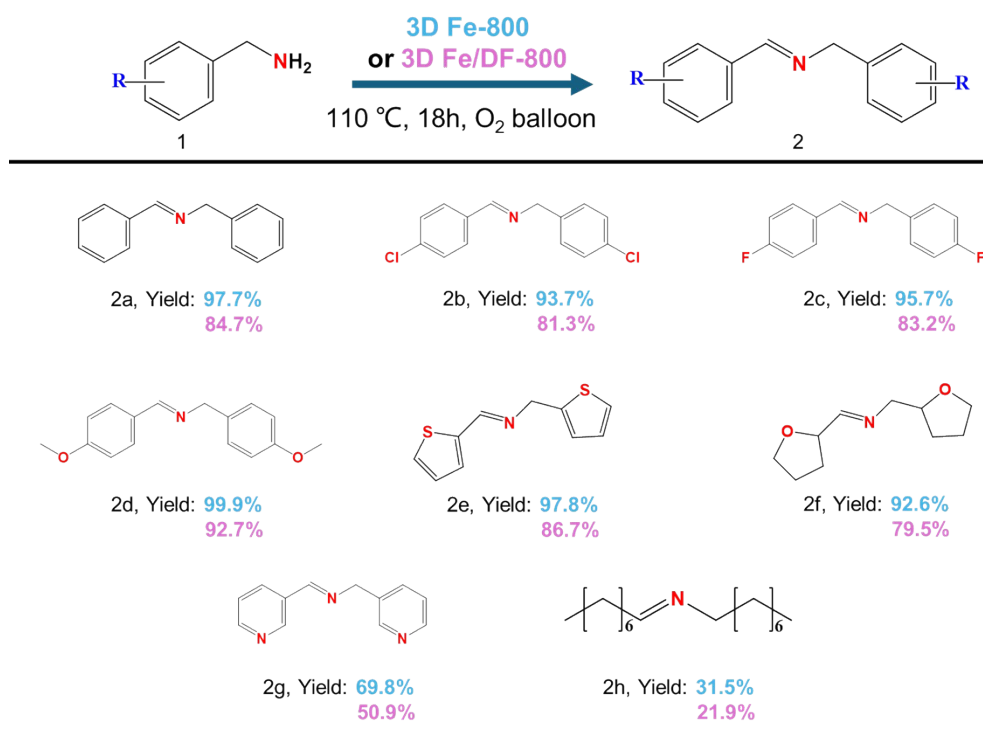
Entry	Catalyst	Conversion (%)	Selectivity (%)	Imine Yield (%)
1	No Cat.	16.5	84.5	13.9
2	3D Fe/DF-700	53.5	98.3	52.6
3	3D Fe-700	48.5	95.6	46.4
4	3D Fe/DF-800	86.0	98.5	84.7
5	3D Fe-800	99.5	98.2	97.7
6	3D Fe/DF-900	80.8	97.1	78.5
7	3D Fe-900	90.2	96.3	86.9
8	3D DF-700	64.0	96.6	61.9
9	3D DF-800	48.8	98.2	47.9
10	3D DF-900	50.0	97.5	48.8
11	3D Fe _{0.25} -600-800	86.3	98.8	85.3
12	3D Fe _{0.5} -600-800	92.4	98.3	90.8

^a) Reaction conditions: Unless otherwise specified, the reaction was carried out with 2 mL of benzylamine (18.3 mmol) and a 30 mg catalyst at 110 °C for 18 h under O₂ conditions.

Table S6 Fe loadings of used catalysts determined by ICP-OES.

Entry	Sample	Fe Content (wt.%)
1	Fresh 3D Fe/DF-700	7.1
2	Used 3D Fe/DF-700	4.7
3	Fresh 3D Fe-700	1.5
4	Used 3D Fe-700	1.5
5	Fresh 3D Fe/DF-800	6.7
6	Used 3D Fe/DF-800	5.2
7	Fresh 3D Fe-800	4.0
8	Used 3D Fe-800	4.0

Table S7 Oxidative coupling of various amines to imines over 3D Fe/DF-800 and 3D Fe-800^a.



^a Reaction conditions: amines (18.3 mmol), catalyst (30 mg), O₂ balloon, 110 °C and 18 h.